INEL-95/00069
CONF-950785

OPTICAL LOCK-IN VIBRATION DETECTION USING PHOTOREFRACTIVE FOUR-WAVE MIXING

Tom Chatters
Ken Telschow

Idaho National Engineering Laboratory
Lockheed Idaho Technologies Co.
P.O. Box 1625
Idaho Falls, Idaho 83415-2209

INTRODUCTION

Many important applications for photorefractive crystals (PRCs) have been found recently by various investigators [1-3]. These applications range from volumetric information storage in optical computing to adaptive, remote detection of ultrasonic vibration in optical nondestructive evaluation [4]. In this paper, we propose the use of PRCs for lock-in detection of continuously vibrating structures.

A method for achieving lock-in detection using the photorefractive effect was presented by Khoury et al of Rome Laboratory in 1991 [5]. They described a technique for the purpose of extracting a small signal phase modulation embedded in a large noise environment. This was carried out by mixing two optical beams, a signal and a reference, with different phase modulation in a photorefractive medium. They presented a first-step analytical model that described the temporal behavior of a photorefractive lock-in device, along with experimental verification of this behavior. The effects of varying different mixing parameters were described qualitatively.

Here, we explore the optical lock-in technique for application in vibration detection and, in particular, its potential for narrowband vibration mode spectral analysis. In addition, we have performed a shot-noise limited signal-to-noise ratio analysis of this device to determine its minimum detectable displacement sensitivity, and simulated the lock-in spectrum analysis method.

EXPERIMENTAL SETUP

The wave mixing process for vibration detection using a photorefractive crystal of BSO ($B_{12}SiO_{20}$) is shown in figure 1. In this setup, the interference of signal beam I_1 and reference beam I_2 generates a space-charge field that modulates the local refractive index (generates a diffraction grating) within the photorefractive crystal. Counter-propagating

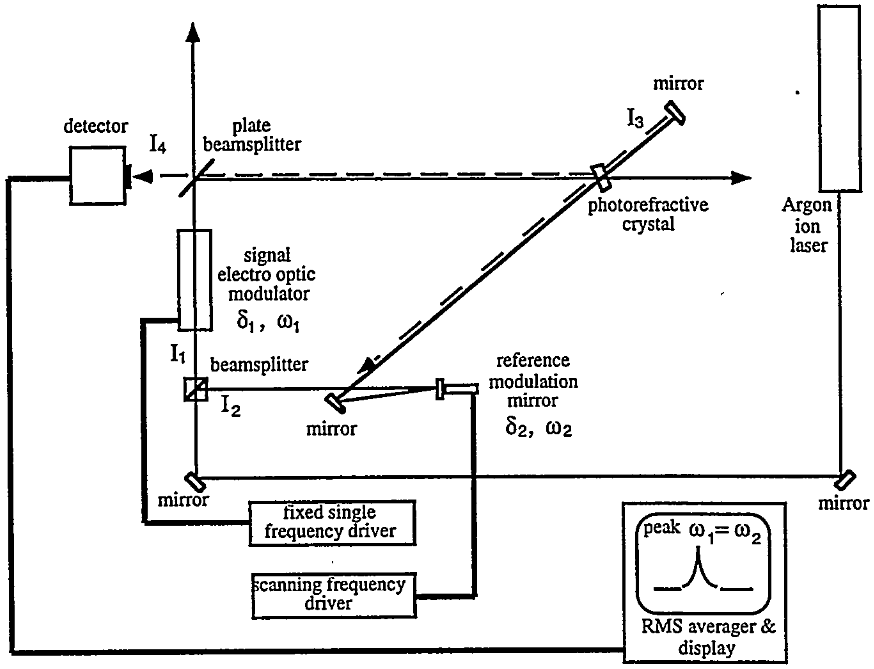

Figure 1 - Optical lock-in detection setup using photorefractive four-wave mixing.

readout beam I_3, antiparallel to reference beam I_2, is sent back into the crystal and, upon diffraction by its passage through the grating in the PRC, generates conjugate beam I_4. The amplitude of conjugate beam I_4 is dependent on the mixing process and is proportional to the amplitude of the space-charge field. Ideally, readout beam I_3 should be incoherent with beams I_1 and I_2 such that these two mixing waves form the only grating in the medium, making the so-called single grating approximation applicable. In this case, the time dependent behavior of this single, primary space-charge field is governed by the time response of the material and the instantaneous phase and intensity of the mixing waves.

LOCK-IN MODEL

To model the lock-in process, the governing equation used for linking the behavior of the space-charge field E_{sc} and the mixing waves A_1 and A_2 is the following first order partial differential equation [5]

$$\frac{\partial E_{sc}}{\partial t} + \frac{E_{sc}}{\tau} = \frac{E_{sc}^{\max}}{\tau} \frac{\left(A_1 \cdot A_2^*\right)}{I_{sat}} \text{ where } E_{sc}^{\max} = \frac{q \rho_o \Lambda}{2\pi\varepsilon} \text{ and } |A_1||A_2| \le I_{sat} \tag{1}$$

and where τ is the material response time and I_{sat} is the light intensity necessary to mobilize all charge carriers within the PRC, saturating the medium. The maximum achievable space-charge field $E_{sc}^{\max}$ is controlled by the concentration of available charge carriers ρ_o, the fringe spacing Λ, the carrier charge q and the permittivitiy of the medium ε [3]. In the lock-in technique, the mixing waves, signal and reference, each have their own unique phase modulation parameters and are given by

$$A_1 = |A_1| e^{[-i\delta_1 \sin(\omega_1 t + \phi_1)]} = |A_1| \sum_{n=-\infty}^{\infty} J_n(\delta_1) e^{[-in(\omega_1 t + \phi_1)]} \tag{2a}$$

$$A_2 = |A_2| e^{[-i\delta_2 \sin(\omega_2 t + \phi_2)]} = |A_2| \sum_{m=-\infty}^{\infty} J_m(\delta_2) e^{[-im(\omega_2 t + \phi_2)]} \tag{2b}$$

where δ_1, ω_1, ϕ_1 and δ_2, ω_2, ϕ_2 are the amplitudes (in radians), frequencies, and phases of the phase modulations imposed by the electro-optic modulator (signal) and the piezo-electric mirror (reference), respectively. Making the same assumption as Khoury et al about the low-pass filtering behavior of the PRC, that it is only capable of responding to the first few frequency difference components of the optical interference occurring within the response time of the material, the space-charge field becomes [5]

$$E_{sc}(t) = E_{sc}^{\max} \frac{|A_1||A_2|}{\tau\, I_{sat}} \sum_{n=-\infty}^{\infty} \frac{J_n(\delta_1) J_n(\delta_2)}{in\Delta\omega + 1/\tau} e^{(-in\Delta\omega t)}\; e^{(-in\Delta\phi)} \tag{3}$$

where $\Delta\omega$ is the frequency difference, $\Delta\phi$ is the phase difference, and J is the Bessel function of the first kind. The space-charge field can then be related to modulation of the local refractive index through the linear electro-optic effect [6]. This effect gives rise to an important parameter in diffractive optics known as the wave coupling constant. Since this quantity is a function of time, we call it the 'wave coupling parameter' and denote it as

$$\nu = \frac{\pi N^3 r_{41} L}{2 \lambda \cos\theta} E_{sc}(t) \tag{4}$$

where N is average refractive index of the medium, r_{41} is the effective, orientation-dependent electro-optic coefficient in BSO, L is the interaction length, λ is the source wavelength, and θ is the angle between the mixing waves. Wave coupling in this lock-in model occurs between the readout beam I_3 and the diffracted (generated) beam I_4, while the signal and reference beams act simply to generate the spatially modulated refractive index (coupling effects between these waves are ignored). The intensity of beam I_4 is related to the coupling parameter and has been well described by Kogelnik [7]

$$I_4 = I_3\, e^{(-2\alpha L/\cos\theta)} (\sin\nu)(\sin\nu)^* \tag{5}$$

where α is the material absorption. In the next step of the analysis, the approximation $\sin\nu\ \sin\nu^* \sim \nu\,\nu^*$ is made since the refractive index modulation amplitude generated in the mixing process is small compared to the average index of the medium. From equations (3) (space-charge field), (4) (wave coupling parameter), and (5) (grating diffraction), and analyzing only the summation terms of n equal to -1, 0, and 1, yields a solution for the intensity of conjugate beam I_4 given by

$$I_4 = C_o\, I_3 \left\{ \frac{C_1^2 L^2}{\tau^2} \left[\tau^2 J_0^2(\delta_2) + \frac{2\,\tau\,\delta_1 J_0(\delta_2) J_1(\delta_2)}{1/\tau^2 + \Delta\omega^2} F + \frac{\delta_1^2 J_1^2(\delta_2)}{(1/\tau^2 + \Delta\omega^2)} F^2 \right] \right\} \tag{6}$$

$$where\ F = 1/\tau \cos(\Delta\omega t + \Delta\phi) - \Delta\omega \sin(\Delta\omega t + \Delta\phi) \tag{7a}$$

$$C_0 = e^{(-2\alpha L/\cos\theta)}\ and\ C_1 = \frac{N^3\, r_{41}\, q\, \rho_o\, \Lambda\, |A_1||A_2|}{4\,\lambda\,\varepsilon \cos\theta\, I_{sat}} \tag{7b \& c}$$

Here, we have only used the first term in the series representation of the Bessel functions with δ_1 arguments.

Inspection of equation (6) shows that the intensity of beam I_4 is made up of a DC offset intensity term, an AC beat intensity term, and a higher order term. The effects of reference beam modulation amplitude δ_2 on the DC and AC intensity components can now be investigated, neglecting the effects on the higher order term. The DC operating intensity is given by

$$\overline{I_4} = C_o\, C_1^2\, I_3\, L^2\, J_0^2(\delta_2) \tag{8}$$

or the first term in equation (6). The DC offset or operating intensity is important since this determines the shot-noise level in the detector while monitoring the beat intensity. From equation (6) the signal peak-to-peak intensity or beat intensity is given by

$$\Delta I_4 = 2\,\delta_1\, C_o\, I_3\, C_1^2\, L^2\, \frac{J_0(\delta_2)J_1(\delta_2)}{1+\Delta\omega^2\tau^2}\,\tau F \tag{9}$$

EXPERIMENTAL RESULTS

In this section, the validity of the lock-in model presented above is explored with respect to the effects of phase modulation amplitude. In the experimental procedure the phase modulation amplitude of the signal beam δ_1, controlled by the electro-optic device, was held constant at a 1/10th of a wave while the amplitude of the reference beam δ_2 was incremented. Also, the signal beam and reference beam were continuously phase modulated at 5 kHz and 5.05 kHz, respectively, maintaining a frequency difference between the two mixing waves of 50 Hz. After detection of the conjugate beam intensity by the photodetector, an adjustable filter was used to select either the DC or AC component of the output signal. The DC offset intensity was obtained by setting up the adjustable filter as a low-pass device with a corner frequency of approximately 10 Hz. The reference beam phase modulation amplitude δ_2 was varied by fractions of an optical wavelength using a calibrated piezo-electric translation mirror. The intensity results of this experiment have been normalized and compared with equation (8) (the solid line) in figure 2. The results show agreement with the analytical model and that large phase incursions around 1/10th of a wavelength begin to drive the DC offset intensity down.

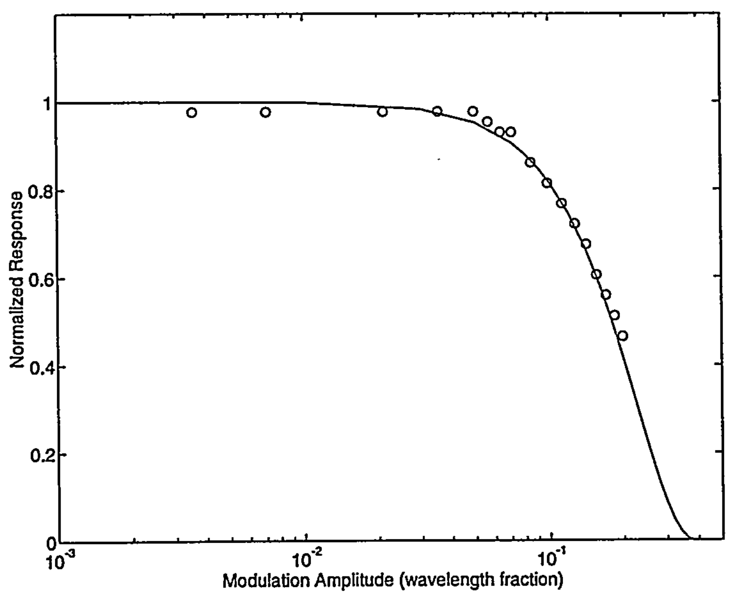

Figure 2 - DC offset intensity compared with prediction of quation (8) (solid line).

Next, the AC beat intensity of the output signal was obtained by setting up the adjustable filter as a high-pass device with a corner frequency of approximately 30 Hz. Again, the reference beam phase modulation amplitude was incrementally varied while the peak-to-peak signal intensity was obtained. The intensity results of this experiment have been normalized and compared to equation (9) in figure 3. The phase modulation amplitude behavior of the AC component in this device agrees with the model. Furthermore, a peak in the experimental data and the model shows that there is an optimum modulation depth for the reference beam at approximately $2/10^{\text{ths}}$ of a wavelength.

VIBRATION MODE SPECTRAL ANALYSIS

The frequency matching character of the device demonstrated suggests that it could be used as a vibration mode spectrum analyzer. This could be done by first configuring the the wave mixing experiment as shown earlier and replacing the electro-optic device with a vibrating specimen and appropriate light collection optics. Then, the frequency of both the signal and reference beam would be swept through the desired range while the output voltage of the detector was put into a RMS averaging device. The output of the averager would then be displayed as a function of frequency, and the display would yield voltage peaks during the frequency scan when the driving frequency matched the vibrational modes of the specimen. Therefore, we are interested in the RMS value of the beat intensity (9), which is given by

$$\Delta I_4 = \sqrt{2}\,\delta_1\,C_o\,I_3\,C_1^2\,L^2\,\frac{J_0(\delta_2)J_1(\delta_2)}{\sqrt{1+\Delta\omega^2\tau^2}} \tag{10}$$

To further illustrate this prospect, we used the analytical model to describe a tuning effect present in equation (10) as a function of frequency difference between the mixing waves. This effect is shown in figure 4 for a system using a PRC with a time response of 0.01 s. The peak in this tuning curve occurs at $\Delta\omega = 0$ and has a full width at half maximum determined by the inverse of the PRC response. The significance of this result is that this device could be used as vibration spectrum analyzer with mode discrimination based on the response time of the crystal used. However, device design issues such as frequency scanning rate become important since a crystal with high discrimination like

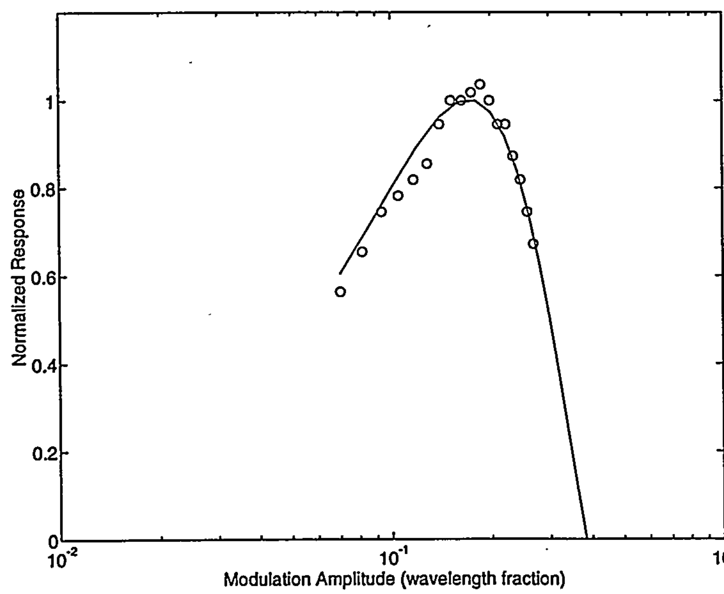

Figure 3 - AC beat intensity compared with the prediction of equation (9) (solid line).

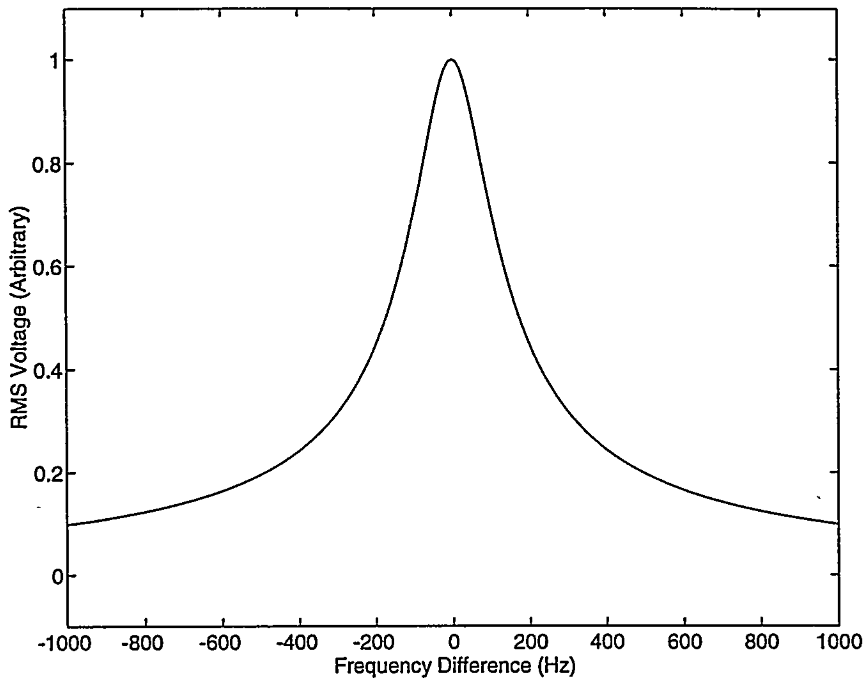

Figure 4 - Simulated vibration mode spectrum, i.e, tuning effect.

$BaTiO_3$ (B equal to 1.0 - 0.1 Hz) requires a relatively slow scan before an adequate response can be detected.

SIGNAL-TO-NOISE RATIO

The shot-noise limited signal-to-noise ratio is given by [8]

$$SNR = C_2 \left(\Delta I_4\right)^2 / \overline{I_4} \text{ where } C_2 = \frac{\eta A}{2 \hbar \nu_p B} \qquad \text{(11a \& b)}$$

and where η is the efficiency of the detector, A is the beam area, $h\nu_p$ is the photon energy of the source, and B is the bandwidth of the crystal. This approach yields a shot-noise limited signal-to-noise ratio given by

$$SNR = 2\, \delta_1^2\, C_o\, C_1^2\, C_2\, I_3\, L^2 \left(\frac{J_1(\delta_2)}{\sqrt{1+\Delta\omega^2\tau^2}} \right)^2 \qquad (12)$$

By setting the signal-to-noise ratio equal to one we can determine the minimum detectable phase modulation δ_{min} given by

$$\delta_{\min} = \frac{1}{\sqrt{2}\, C_1\, L} \frac{\sqrt{1+\Delta\omega^2\tau^2}}{J_1(\delta_2)} \sqrt{\frac{1}{C_o\, C_2\, I_3}} \qquad (13)$$

From inspection, we expect the highest sensitivity of the device to occur with the reference phase modulation amplitude δ_2 equal to 1.841 radians, and this determines the optimum operating configuration for a photorefractive optical lock-in vibration device. As an example of the use of this expression, we define some realistic parameters (listed below for BSO) for the application of this device (operating in saturation and with $\Delta\omega = 0$) and calculate δ_{min} to be $2.77 \cdot 10^{-8}$ radians per $Hz^{1/2}$; for vibration displacement measurements δ_{min} is equal to $1.13 \cdot 10^{-6}$ nm per $Hz^{1/2}$.

$r_{41} = 5*10^{-12}$ ($m \cdot V^{-1}$)	$\varepsilon = 56*8.85*10^{-12}$ ($C^2 \cdot N^{-1} \cdot m^{-2}$)
$\Lambda = 10^{-6}$ (m)	$\rho_o = 10^{22}$ (m^{-3})
$\alpha = 0.0005$ (m^{-1})	$N = 2.54$ (unitless)
$I_3 = 10^6$ ($Watts \cdot m^{-2}$)	$A = 10^{-6}$ (m^2)
$L = 5*10^{-3}$ (m)	$\eta = 30\%$
$\lambda = 514*10^{-9}$ (m)	$h\nu_p = 3.865*10^{-19}$ (Joules)

CONCLUSIONS

An optical lock-in method for vibration mode spectral analysis using photorefractive four-wave mixing has been described, and some of its operating characteristics modeled and measured. The theoretical displacement sensitivity of this optical lock-in vibration mode spectrum analyzer has been demonstrated to be well below the nanometer range. Currently, work is underway to demonstrate the capability of this approach for narrowband vibration mode spectrum analysis.

ACKNOWLEDGMENT

This work is supported through the INEL Laboratory Directed Research & Development Program under DOE Idaho Operations Office Contract DE-AC07-94ID13223.

REFERENCES

1. T.J. Hall, R. Jaura, L.M. Connors and P.D. Foote, " The photorefractive effect: a review", Progress in Quantum Electronics, Vol. 10, pp. 77-146, (1985).

2. R. Saxena, M.J. Rosker, and I. McMichael, "Frequency locking in the photorefractive phase-conjugate ring oscillator", Journal of the Optical Society of America B, Vol. 9, pp. 1735-1743, (September 1992).

3. P. Yeh, Introduction to Photorefractive Nonlinear Optics, John Wiley & Sons, Inc., (1993).

4. A. Blouin and Jean-Pierre Monchalin, "Detection of ultrasonic motion of a scattering surface by two-wave mixing in a photorefractive GaAs crystal", Applied Physics Letters, Vol. 65, No. 8, (1994).

5. J. Khoury,V. Ryan, C. Woods and M. Cronin-Golomb, "Photorefractive optical lock-in detector", Optics Letters, Vol. 16, pp. 1442-1444, (September 1991).

6. N.V. Kukhtarev, V.B. Markov, S.G. Odulov, M.S. Soskin and V.L. Vinetskii, "Holographic storage in electrooptic crystals. I. Steady State", Ferroelectrics, Vol. 22, pp. 949-960, (1979).

7. H. Kogelnik,"Coupled wave theory for thick hologram gratings", The Bell System Technical Journal", Vol. 48, pp. 2909-2947, (November 1969).

8. J.W. Wagner, "Optical detection of ultrasound," Ultrasonic Measurement Methods, Eds. R.N. Thurston and A.D. Pierce, Academic Press, Ch. 5, (1990).